TN update plans and advances for ^{16}O and ^{9}Be

Cross Section Evaluation Working Group
Evaluations Committee
G. Hale & M. Paris (LANL/T-2)

2021-11-18

LA-UR-21-31398

Outline

- Thermonuclear/charged-particle evaluation updates
- n+^{9}Be status & plans
- n+^{16}O progress report

Thermonuclear/charged-particle reactions

Detailed in earlier Charged-particle session 2021-11-17

- Evaluation updates & new evaluations
  - `p-001_H_001.endf`
  - `p-002_He_004.endf`
  - `d-001_H_003.endf`
  - `d-002_He_003.endf`
  - `d-003_Li_006.endf`
  - `t-002_He_004.endf`
  - `a-006_C_013.endf`

n+^{9}Be evaluation

Light-element R-matrix evaluation

R-matrix formalism

Exterior region

$$|\Psi_c^{(+)}\rangle = |\mathscr{I}_c\rangle - \sum_{c'} |\mathscr{O}_{c'}\rangle S_{c'c}$$

$$S_{cc'} = \delta_{cc'} + 2i\, T_{cc'}$$

$r \to \infty$

Channel surface

$\mathscr{S}_c \in \mathbb{R}^{3A-4}$

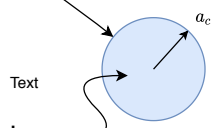

Interior region

$$[H + \mathscr{L}_B]\,|\lambda\rangle = E_\lambda |\lambda\rangle$$

$$|\Psi^{(+)}\rangle = [H + \mathscr{L}_B - E]^{-1}\mathscr{L}_B |\Psi^{(+)}\rangle$$

$$\mathscr{L}_B = \sum_c \frac{ia_c}{2m_c} |a_c\rangle\langle a_c|(\hat{p}_r + iB_c)$$

$$R_{B,c'c} = \langle c'|[H + \mathscr{L}_B - E]^{-1}|c\rangle = \sum_\lambda \frac{\langle c'|\lambda\rangle\langle\lambda|c\rangle}{E_\lambda - E}$$

EDA R-matrix evaluation procedure

R-matrix

$$R_{c'c} = \sum_\lambda \frac{\gamma_{\lambda,c'}\gamma_{\lambda,c}}{E_\lambda - E}$$

Initial guess:

$$\mathbf{p}^{(0)} = \{E_\lambda^{(0)}, \gamma_{\lambda,c}^{(0)}\}$$

T-matrix

$$T = -O^{-1}F + O^{-1}R_L O^{-1}$$

$$R_L^{-1} = R^{-1} + B - L$$

Observables

$$\rho_f = T\rho_i T^\dagger$$

$$X_{i_M}(\mathbf{p}) \propto \langle O_f\rangle = \frac{\mathrm{Tr}\ \rho_f O_f}{\mathrm{Tr}\ \rho_f}$$

Data

e.g. EXFOR/CSIRS

Processes: elastic, inelastic, transfer, break-up,...

Unpolarized:

$\sigma_{\mathrm{tot}}(E), \sigma(E), d\sigma/d\Omega(E,\theta)$

Polarized: $P_y, A_y, C_{x,x'}, \ldots$

Optimize

$$\chi^2_{\mathrm{EDA}}(\mathbf{p}) = \sum_{M,i_M}\left[\frac{n_M X_{i_M}(\mathbf{p}) - R_i}{\Delta R_{i_M}}\right]^2 + \left[\frac{n_M S_M - 1}{\Delta S_M / S_M}\right]^2$$

$$|\nabla_{\mathbf{p}}\chi^2_{\mathrm{EDA}}(\mathbf{p})| \overset{?}{<} \epsilon$$

NO

YES

Solution/Postprocessing

1) Construct ENDF-6 formatted evaluated data file

2) Covariance data

3) Post-process break-up spectra with `SPECT` code

n+^{9}Be
New evaluation

- Added data: elastic, (n,α), (n,n$_1$)

Channel	a_c(fm)	$\ell_{\max}$
$n+^9\mathrm{Be}(\frac{3}{2}^-)$	4.67	3
$^4\mathrm{He}+^6\mathrm{He}(0^+)$	5.00	4
$(nn)_0+^8\mathrm{Be}(2^+)$	5.20	3
$n+^9\mathrm{Be}^*(\frac{5}{2}^-)$	5.20	1

Process	E_n range	Observables	N_{dat}	χ^2/N_{dat}
$^9\mathrm{Be}(n,n_0)^9\mathrm{Be}$	(1.25 eV, 15.4 MeV)	$\sigma_{\mathrm{tot}}, \sigma, \sigma(\theta), A_y(\theta)$	5782	1.65
$^9\mathrm{Be}(n,{}^4\mathrm{He})^6\mathrm{He}$	(0.63, 8.5) MeV	$\sigma, \sigma(\theta)$	178	1.40
$^9\mathrm{Be}(n,2n)^8\mathrm{Be}$	(1.8, 14.7) MeV	σ	40	NA
$^9\mathrm{Be}(n,n_1)^9\mathrm{Be}^*$	(2.7, 5.0) MeV	$\sigma(\theta)$	83	1.65
Total			6083	1.75

n+^{9}Be Integrated Cross Sections

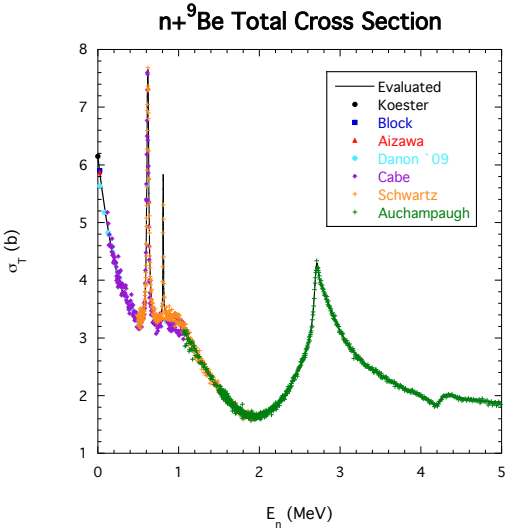

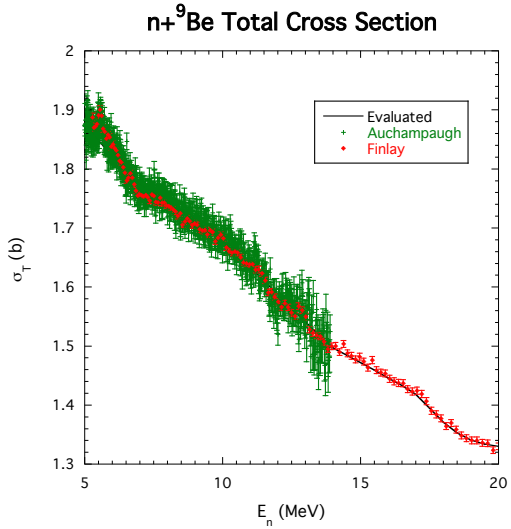

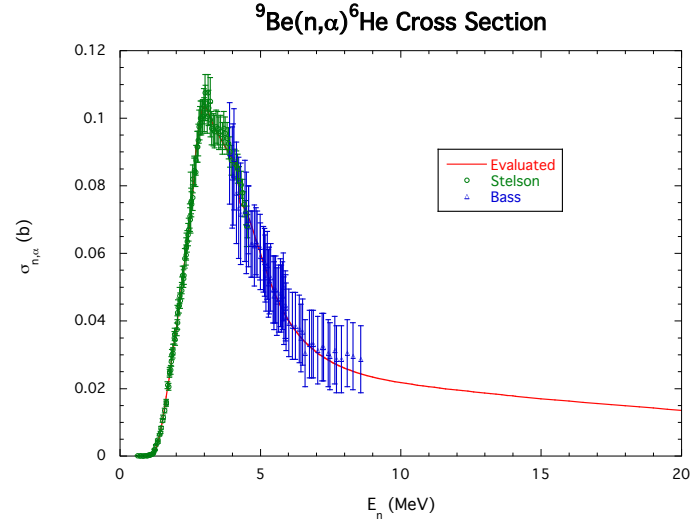

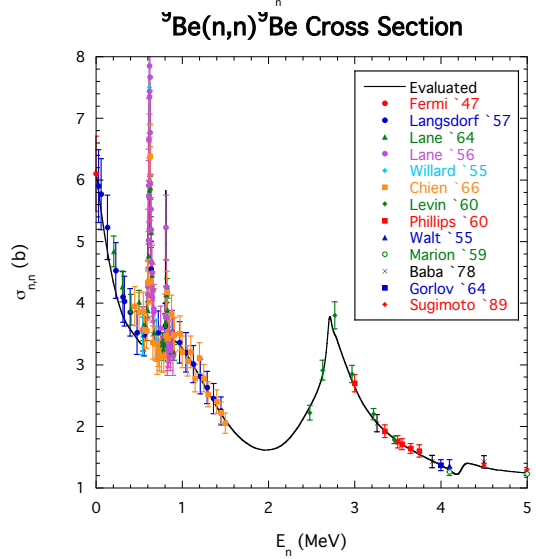

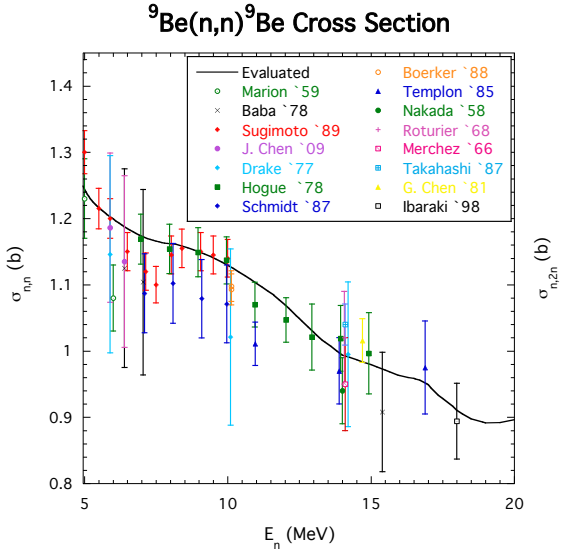

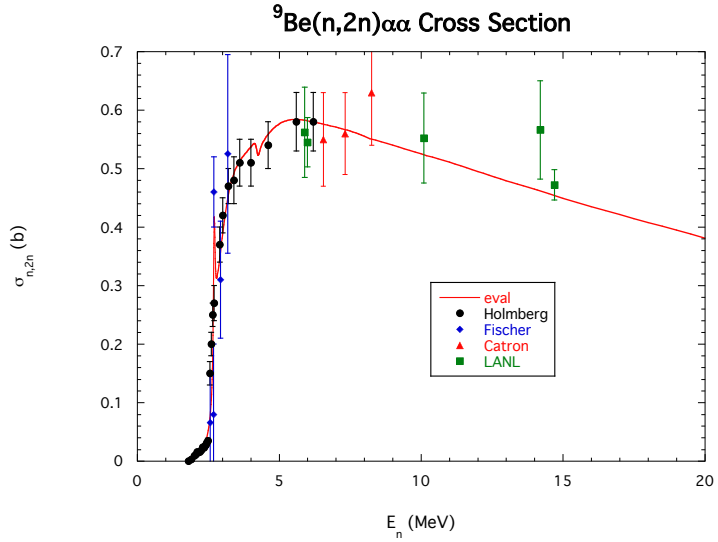

^{9}Be(n,n)^{9}Be Differential Cross Sections

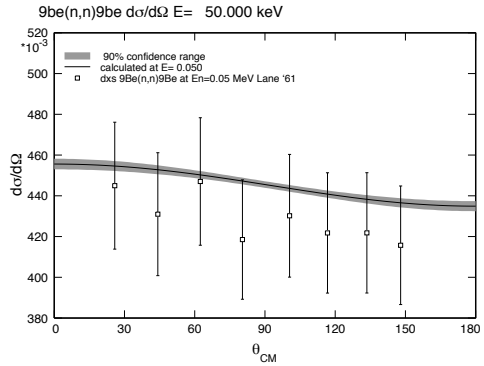

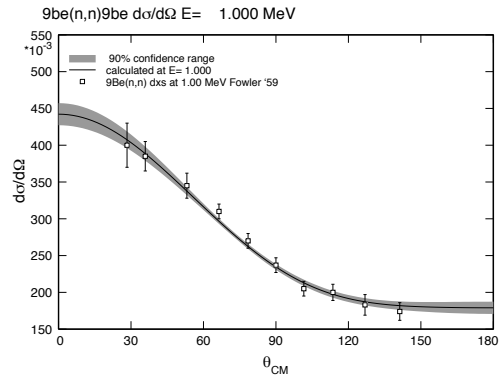

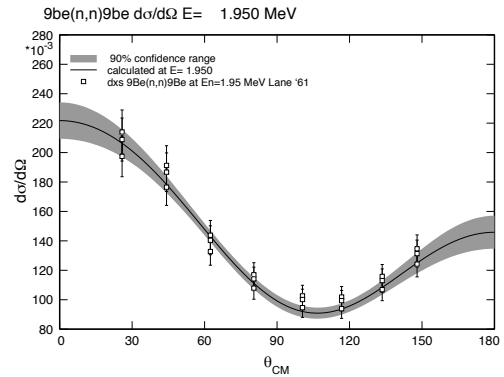

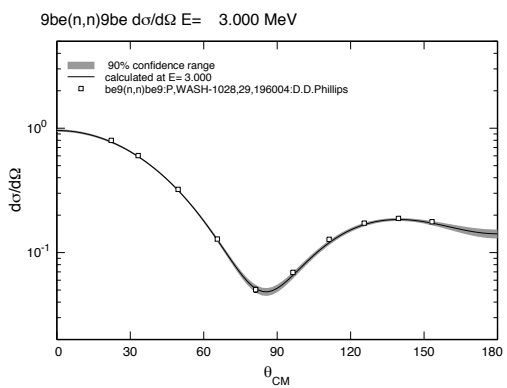

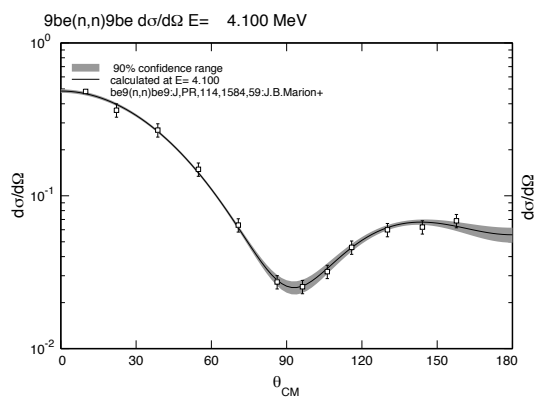

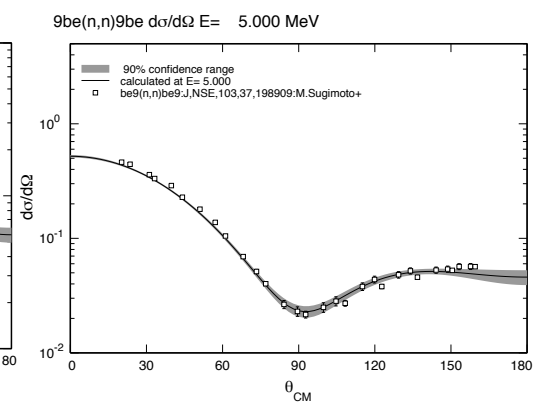

$^{9}Be(n,n_1)^{9}Be^{*}$ Differential Cross Sections

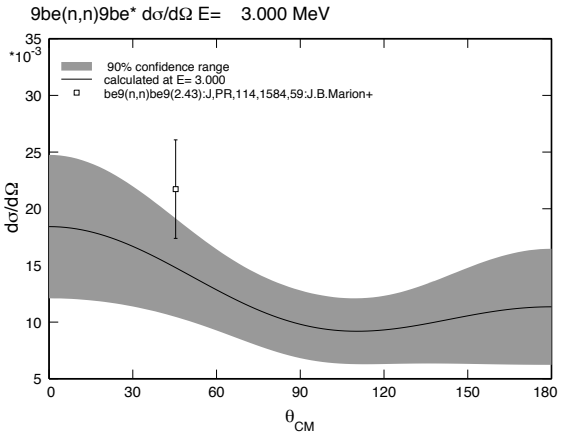

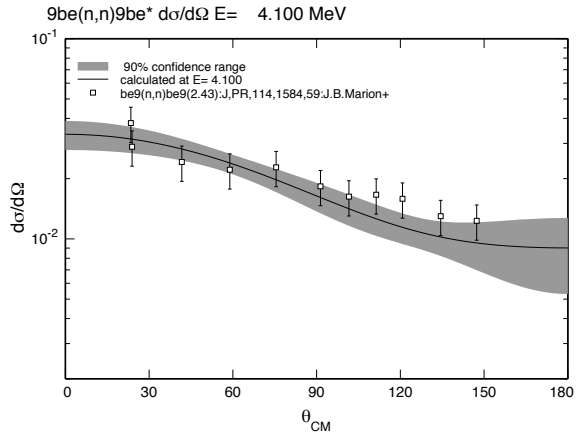

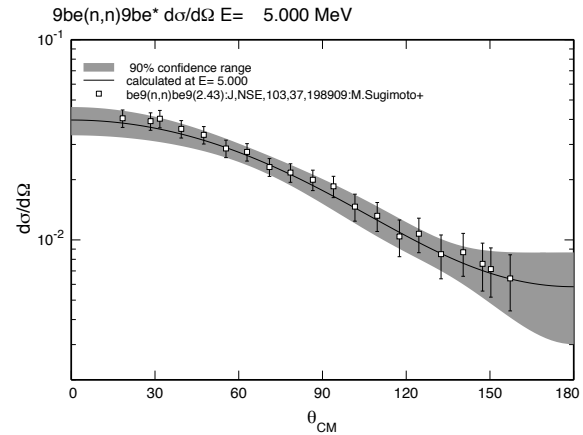

Summary of new evaluation:

- ^{10}Be analysis has produced a consistent set of cross sections and angular distributions that are in agreement with most of the experimental data at energies up to 5 MeV. Extensions above that energy were based on the experimental data alone.
- Level assignments for the overlapping resonances near E_n=2.7 MeV have the opposite parity ($4^-,3^+ \rightarrow 4^+,3^-$).
- Excited states of ^{9}Be make important contributions to the (n,2n) cross section (MT=16 → 24 in the new evaluation).
- Testing/benchmarking: (M. Herman, LANL) and thick-target angular neutron yields (Y. Danon, RPI) on the following slides

Comparison to previous ENDF/B

Integrated cross sections

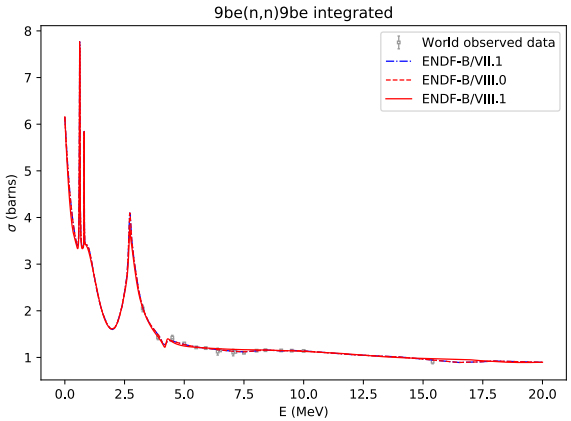

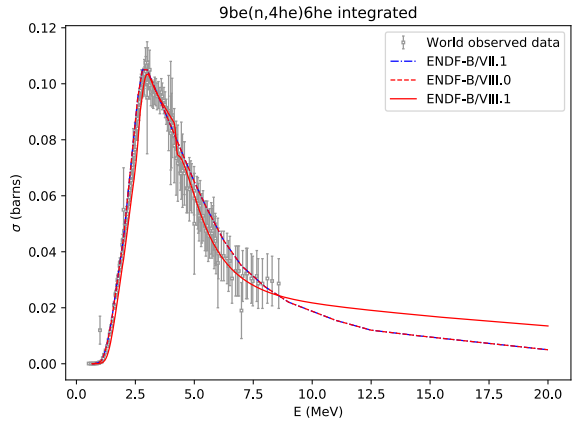

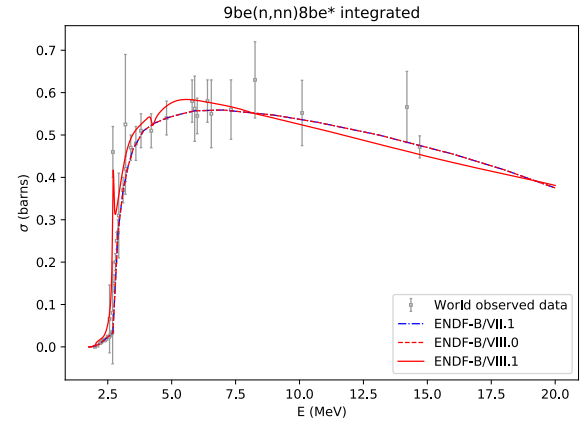

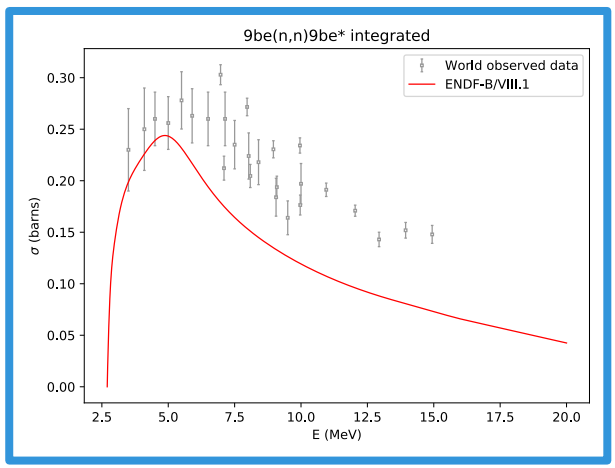

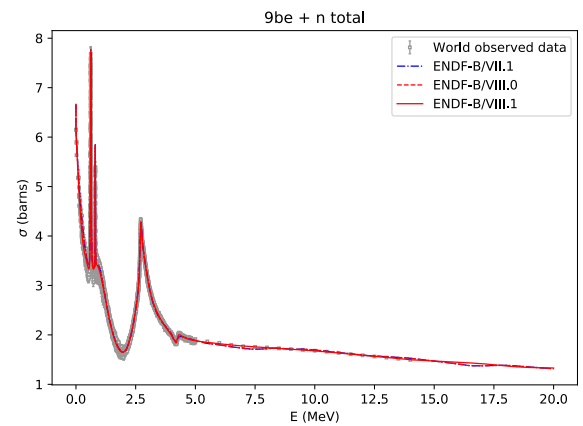

Testing/benchmarks
Pencil-beam study

- K. Parsons/LANL

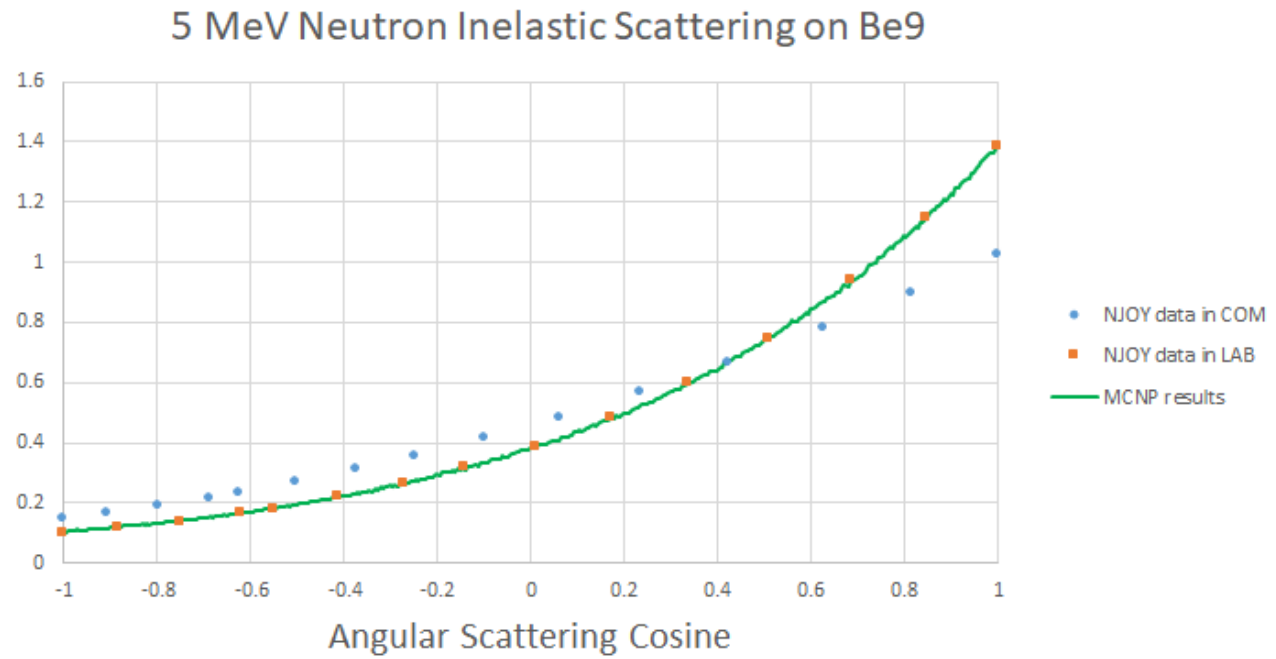

Testing/benchmarks
Lab spectra

- Theoretical model expectation (G. Hale/LANL)

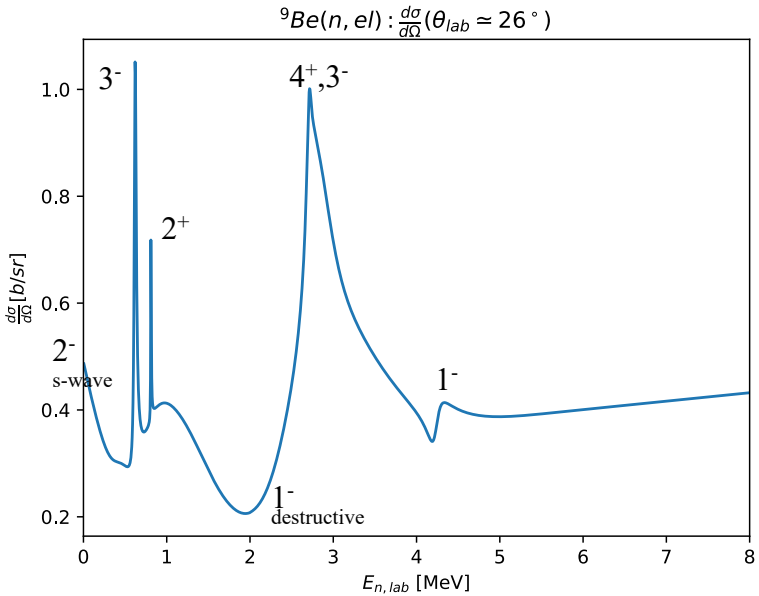

Lab elastic diff. scattering cross section *excitation function* (b/sr) at 26° as a function of E, the incident lab neutron energy (MeV).

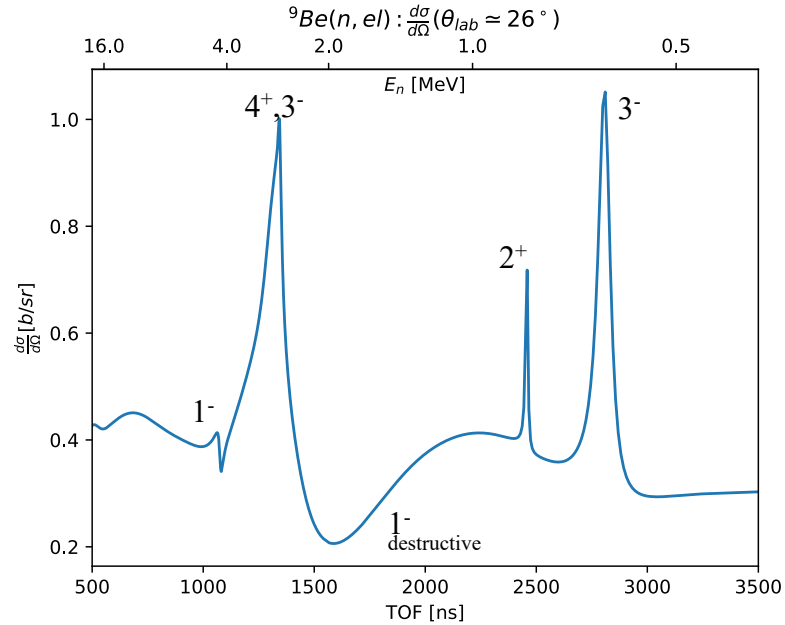

Outgoing neutron TOF spectrum at 26° vs. **t= 2236/sqrt(E)** in ns. Incident energy (top axis), the first two resonances give structures at about 2400 and 2800 ns.

Testing/benchmarks
Lab spectra

- Quasi-integral simulation in MCNP (Y. Danon/RPI)

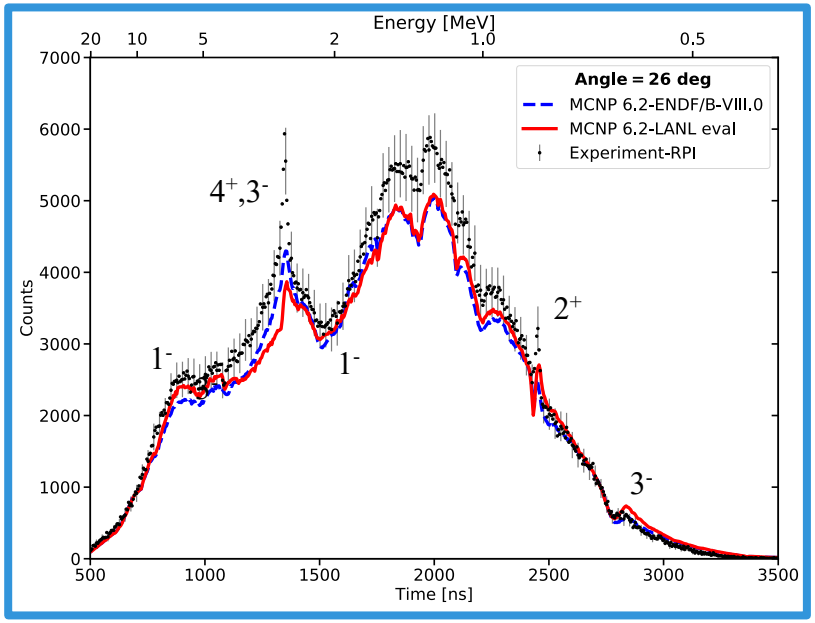

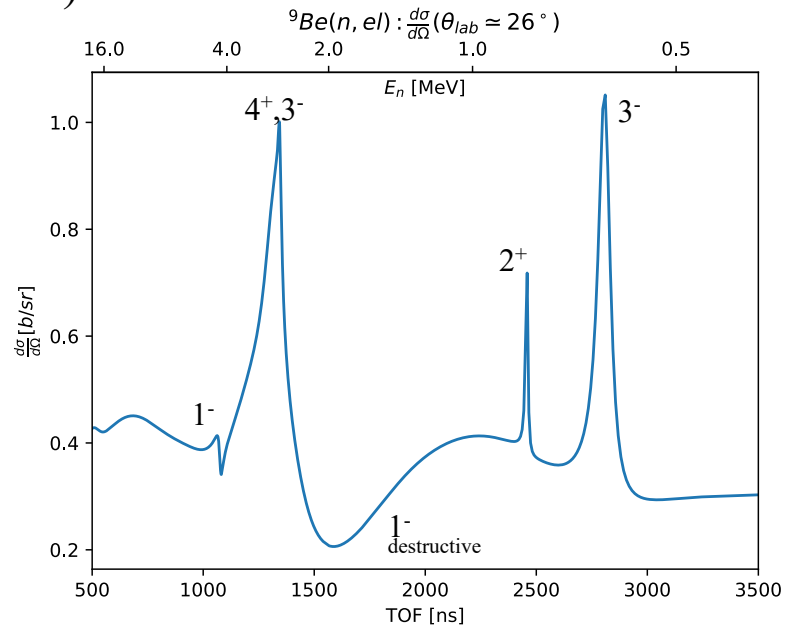

Outgoing neutron TOF spectrum at 26° vs. **t= 2236/sqrt(E)** in ns. Incident energy (top axis), the first two resonances give structures at about 2400 and 2800 ns.

Testing/benchmarks

Pulsed Be spheres

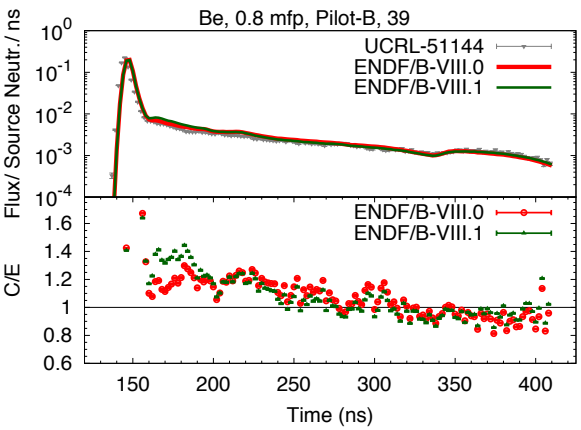

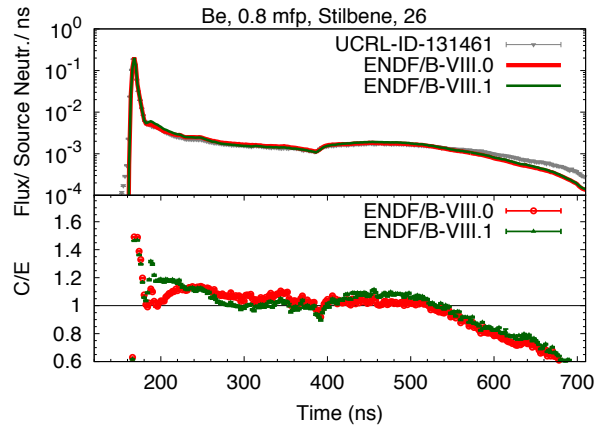

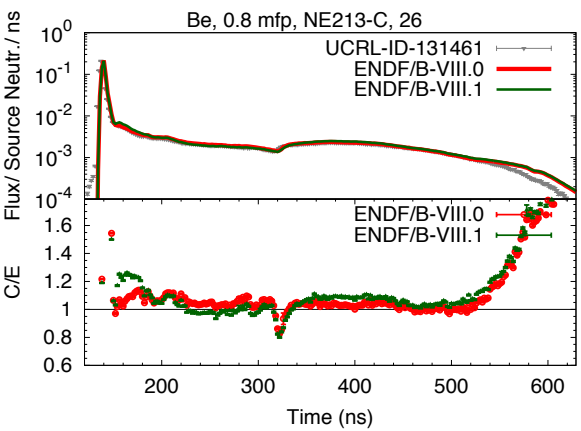

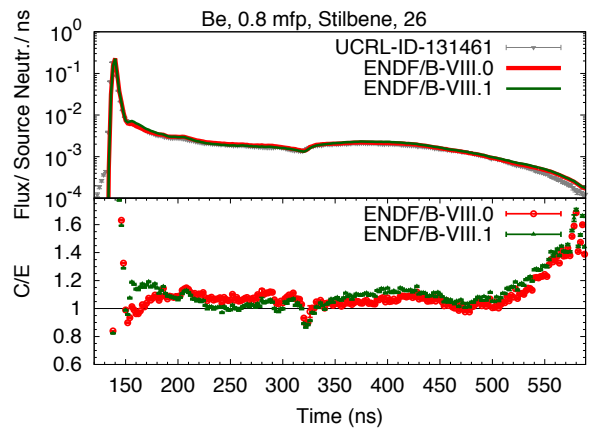

- MCNP simulations (D. Neudecker/LANL)
  - Due to change (n,2n) & (n,n') evident near elastic peak
  - (n,2n) should probably be (has not been) reduced by (n,n')

Perturbative criticality study

M. Herman & W. Haeck (LANL)

Reaction: Be9 (n, elastic)

121 experiments with absolute change > 10.0 pcm

St. Deviation Old: 1111 pcm

St. Deviation New: 1172 pcm

Average Bias Old: -571 pcm

Average Bias New: -678 pcm

Benchmark Name	Diff. (pcm)	Old (pcm)	New (pcm)
HEU-MET-FAST-005-002	−86	−288	−374
HEU-MET-FAST-005-003	−129	−4	−133
HEU-MET-FAST-005-004	−148	−600	−748
HEU-MET-FAST-005-005	−74	−19	−93
HEU-MET-FAST-005-006	−41	−172	−213
HEU-MET-FAST-010-001	−40	−133	−173
HEU-MET-FAST-010-002	−21	−202	−223
HEU-MET-FAST-016-001	−95	69	−26
HEU-MET-FAST-016-002	−50	161	111
HEU-MET-FAST-017-001	−83	−56	−139
HEU-MET-FAST-030-001	−65	78	13
HEU-MET-FAST-038-001	−60	125	65
HEU-MET-FAST-038-002	−43	161	118
HEU-MET-FAST-041-001	−129	350	221
HEU-MET-FAST-041-002	−186	14	−172
HEU-MET-FAST-052-001	−56	388	332
HEU-MET-FAST-058-001	−207	21	−186
HEU-MET-FAST-058-002	−172	241	69
HEU-MET-FAST-058-003	−137	78	−59
HEU-MET-FAST-058-004	−103	8	−95
HEU-MET-FAST-058-005	−79	−48	−127
HEU-MET-FAST-059-001-s	−23	−253	−276
HEU-MET-FAST-059-002-s	−15	−221	−236
HEU-MET-FAST-066-001	−183	−208	−391
HEU-MET-FAST-066-002	−147	−285	−432
HEU-MET-FAST-066-003	−125	−	−125
HEU-MET-FAST-066-004	−220	−235	−455
HEU-MET-FAST-066-005	−187	−133	−320
HEU-MET-FAST-066-006	−160	−164	−324
HEU-MET-FAST-066-007	−192	−188	−380
HEU-MET-FAST-066-008	−218	−201	−419
HEU-MET-FAST-066-009	−182	−221	−403
HEU-MET-FAST-069-001-s	−32	−110	−142
HEU-MET-FAST-070-002	−14	89	75
HEU-MET-FAST-084-003	−92	−86	−178
HEU-MET-FAST-084-016	−55	−108	−163
HEU-MET-FAST-084-026	−55	60	5
HEU-MET-FAST-084-027	−59	−229	−288
HEU-MET-FAST-094-001	−71	206	135

Benchmark Name	Diff. (pcm)	Old (pcm)	New (pcm)
HEU-MET-FAST-094-002	−59	261	202
HEU-MET-MIXED-012-001	−17	505	488
MIX-MET-FAST-004-001	−30	46	16
MIX-MET-FAST-004-002	−16	−68	−84
MIX-MET-FAST-007-001	−179	79	−100
MIX-MET-FAST-007-002	−175	567	392
MIX-MET-FAST-007-003	−146	423	277
MIX-MET-FAST-007-004	−118	347	229
MIX-MET-FAST-007-005	−78	129	51
MIX-MET-FAST-007-006	−46	21	−25
MIX-MET-FAST-007-007	−188	418	230
MIX-MET-FAST-007-008	−173	311	138
MIX-MET-FAST-007-009	−162	299	137
MIX-MET-FAST-007-010	−125	308	183
MIX-MET-FAST-007-011	−98	201	103
MIX-MET-FAST-007-012	−57	142	85
MIX-MET-FAST-007-013	−24	21	−3
MIX-MET-FAST-007-014	−169	600	431
MIX-MET-FAST-007-015	−155	570	415
MIX-MET-FAST-007-016	−115	427	312
MIX-MET-FAST-007-017	−84	441	357
MIX-MET-FAST-007-018	−43	685	642
MIX-MET-FAST-007-019	−104	542	438
MIX-MET-FAST-007-020	−71	370	299
MIX-MET-FAST-007-021	−25	431	406
MIX-MET-FAST-007-022	−92	270	178
MIX-MET-FAST-007-023	−57	251	194
PU-MET-FAST-018-001	−138	−185	−323
PU-MET-FAST-019-001	−139	25	−114
PU-MET-FAST-021-001	−109	353	244
PU-MET-FAST-021-002	−59	−769	−828
PU-MET-FAST-038-001-d	−162	24	−138
PU-MET-FAST-044-003	−67	89	22
U233-MET-FAST-005-001	−90	−235	−325
U233-MET-FAST-005-002	−133	−277	−410
U233-SOL-INTER-001-001	−192	−1816	−2008
U233-SOL-INTER-001-002	−162	−2230	−2392
U233-SOL-INTER-001-003	−142	−2137	−2279
U233-SOL-INTER-001-004	−64	−889	−953

Benchmark Name	Diff. (pcm)	Old (pcm)	New (pcm)
U233-SOL-INTER-001-005	−115	−1767	−1882
U233-SOL-INTER-001-006	−31	−1540	−1571
U233-SOL-INTER-001-007	−93	−2016	−2109
U233-SOL-INTER-001-009	−60	−2298	−2358
U233-SOL-INTER-001-010	−66	−2312	−2378
U233-SOL-INTER-001-011	−32	−2171	−2203
U233-SOL-INTER-001-012	−189	−2188	−2377
U233-SOL-INTER-001-013	−166	−2097	−2263
U233-SOL-INTER-001-015	−139	−2276	−2415
U233-SOL-INTER-001-017	−63	−1270	−1333
U233-SOL-INTER-001-018	−113	−2392	−2505
U233-SOL-INTER-001-019	−90	−2722	−2812
U233-SOL-INTER-001-021	−64	−2945	−3009
U233-SOL-INTER-001-022	−42	−2415	−2457
U233-SOL-INTER-001-024	−193	−1119	−1312
U233-SOL-INTER-001-025	−165	−1789	−1954
U233-SOL-INTER-001-026	−145	−1422	−1567
U233-SOL-INTER-001-028	−115	−1903	−2018
U233-SOL-INTER-001-029	−91	−2535	−2626
U233-SOL-INTER-001-031	−72	−1179	−1251
U233-SOL-INTER-001-032	−42	−2685	−2727
U233-SOL-THERM-015-001	−195	−1354	−1549
U233-SOL-THERM-015-002	−168	−1763	−1931
U233-SOL-THERM-015-004	−61	−1241	−1302
U233-SOL-THERM-015-011	−195	−1013	−1208
U233-SOL-THERM-015-012	−169	−944	−1113
U233-SOL-THERM-015-013	−149	−1136	−1285
U233-SOL-THERM-015-014	−59	−405	−464
U233-SOL-THERM-015-015	−121	−1330	−1451
U233-SOL-THERM-015-016	−101	−1421	−1522
U233-SOL-THERM-015-018	−69	−2831	−2900
U233-SOL-THERM-015-019	−46	−2771	−2817
U233-SOL-THERM-015-020	−200	−807	−1007
U233-SOL-THERM-015-021	−177	−510	−687
U233-SOL-THERM-015-022	−158	−694	−852
U233-SOL-THERM-015-023	−131	−893	−1024
U233-SOL-THERM-015-024	−112	−1186	−1298
U233-SOL-THERM-015-026	−172	−840	−1012
U233-SOL-THERM-015-027	−153	−399	−552
U233-SOL-THERM-015-028	−134	−582	−716
U233-SOL-THERM-015-029	−110	−697	−807
U233-SOL-THERM-015-030	−87	−777	−864
U233-SOL-THERM-015-031	−51	−870	−921

Krusty testing

J. Favorite (LANL/XCP-7)

Case		Benchmark	ENDF/B-VII.1	ENDF/B-VIII.0	ENDF/B-VIII.1
keff					
	1	1.00065	1.00315	1.00043	1.00259
	2	1.00345	1.00597	1.00325	1.00551
	3	1.00017	1.00291	1.00017	1.00240
	4	1.00048	1.00300	1.00033	1.00250
	5	1.00189	1.00441	1.00174	1.00393
C–E					
	1		0.00250	-0.00022	0.00194
	2		0.00252	-0.00020	0.00206
	3		0.00274	0.00000	0.00223
	4		0.00252	-0.00015	0.00202
	5		0.00252	-0.00015	0.00204

"Krusty detailed models compared with the benchmark, ENDF/B-VII.1, and ENDF/B-VIII.0. We nailed it with ENDF/B-VIII.0. The new cross sections are a little better than ENDF/B-VII.1 but not nearly as good as ENDF/B-VIII.0."

n+^{16}O evaluation

ENDF/B history

6.8, 7.1, 8.0

- ENDF/B-VI.8 (2001 April): LANL(Chadwick, Hale, Young), KAPL(Caro, Lubitz)
  - Below 3.4 MeV*: R-*function* + optical model (OPTIC code; Caro)
  - 3.4 < E_n < 6.25: LANL R-matrix (multichannel; EDA)
    - Data: n+^{16}O (total) [Johnson75, Larson80], ^{16}O(n,el) ang.[Lane60,…], ^{16}O(n,α_0) [inverse Walton et al.], ^{13}C(α,n), ^{13}C(α,el) excit. fn
  - E_n > 6.25
    - 6.25 → 20: subtraction of non-elastic (MT=3) from total
    - Inelastic (MT51, …, 57)
      - ^{16}O(n,xγ) Nelson, Chadwick, Michaudon & Young NSE99
  - MT800: Bair&Haas73 without renormalization
    - 6.2→20: factor of 1.5 "bring into rough agreement" (n,α_0) of Davis '63
  - MT801-803: inferred from (n,$\alpha\gamma$) [Nelson99]
- ENDF/B-VII.1 (2005 Dec.): VI.8+Page+Kawano+Young
  - MT=800: 32% reduction (n,α_0) 2.4→8.9 MeV
    - "assuming Harissopulos05 are definitive"; "Ha05 is 100% correct, BH73 100% wrong norm"
- ENDF/B-VIII.0 (2016 Dec.): VII.1+Hale+Kawano+MWP
  - Re-evaluation of Ha05 by Giorginis et al. (CIELO)
- JENDL-4.0 (2010)
  - ^{16}O(n,α_{tot}) < 6.5 MeV ~ ENDF/B-VII.0

*all incident neutron lab energies [MeV]

ENDF/B comparisons $^{16}O(n,\alpha_0)^{13}C$ [MT=800]

6.8, 7.1, 8.0

- Three regions
  - I. < 5.2 MeV
  - II. 5.2 → 6 MeV
  - III. > 6 MeV
- Trends
  - I. 7.1 < 6.8/8.0
  - II.~Equivalent
  - III.7.1 < 6.8 < 8.0

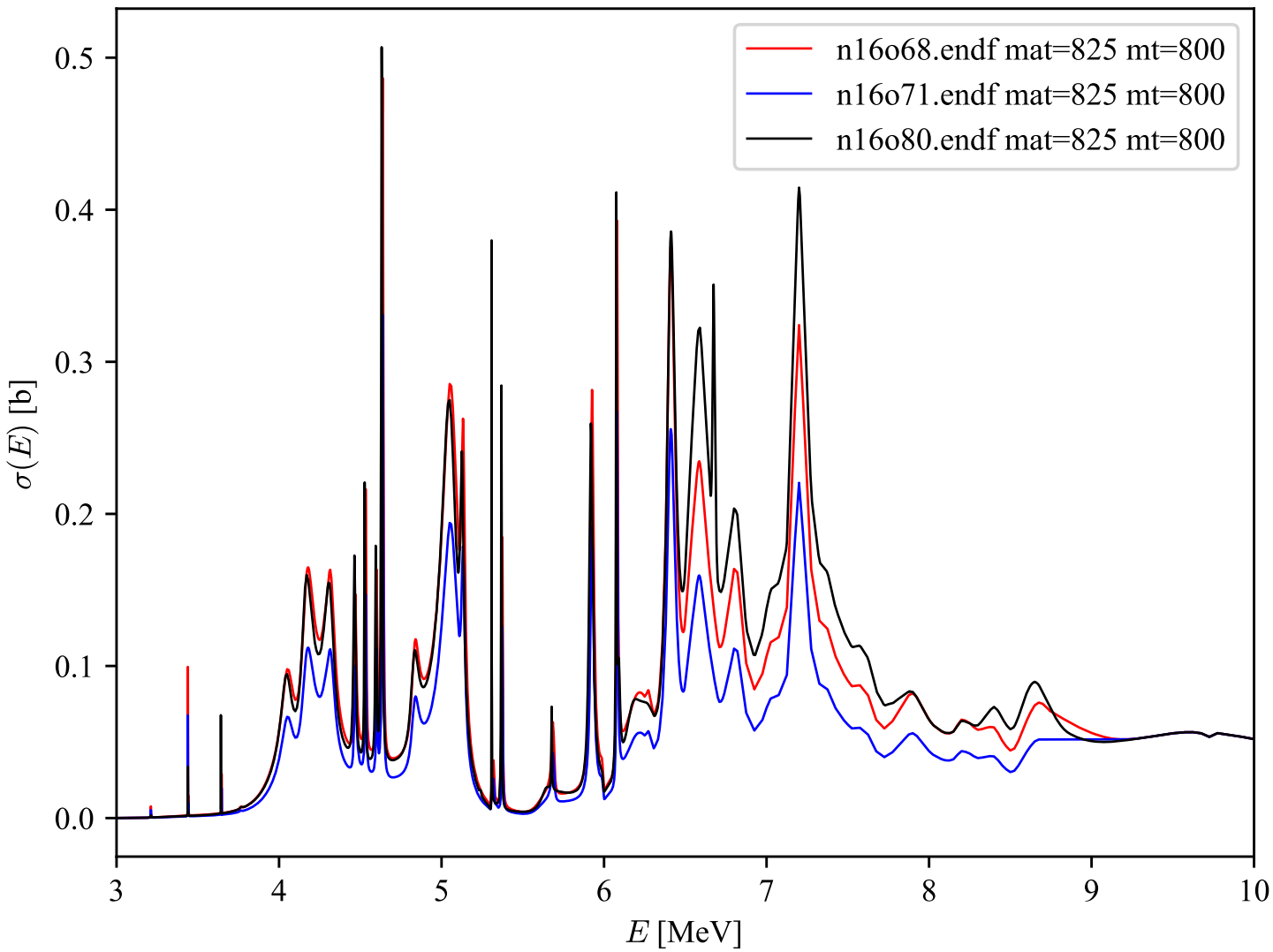

^{17}O Preliminary evaluation

Preliminary results

- Configuration: channels, R-matrix parameters
- Observed data in `data` deck
  - Channels: (n,n_0), (n,n_2), $(\boldsymbol{\alpha},n_0)$, $(\boldsymbol{\alpha},n_1)$, $(\boldsymbol{\alpha},n)$
  - Types: total, integrated, differential, *polarization* $[A_y, P_n]$

Channel	a_c(fm)	$\ell_{\max}$
$n+^{16}\mathrm{O}(0^+;\mathrm{gs})$	4.40	4
$\alpha+^{13}\mathrm{C}(\frac{1}{2}^-;\ \mathrm{gs})$	5.40	5
$n_1+^{16}\mathrm{O}(0^+;\ 6.05\ \mathrm{MeV})$	5.00	3
$n_2+^{16}\mathrm{O}(3^-;\ 6.13\ \mathrm{MeV})$	5.00	2

Reaction	Range E_n, E_α (MeV)	N_{dat}	Observables
$^{16}\mathrm{O}(n,n)^{16}\mathrm{O}$	(0.0, 7.0)	2,909	$\sigma_{\mathrm{tot}}, \sigma,$ $\sigma(\theta), A_y(\theta)$
$^{16}\mathrm{O}(n,n_2)^{16}\mathrm{O}(3^-;\ 6.13\ \mathrm{MeV})$	(6.6, 8.8)	45	$\sigma(\theta)$
$^{13}\mathrm{C}(\alpha,\alpha)^{13}\mathrm{C}$	(2.0, 5.7)	1,397	$\sigma(\theta)$
$^{13}\mathrm{C}(\alpha,n)^{16}\mathrm{O}$	(.23, 8.0)	1,054	σ_r
$^{13}\mathrm{C}(\alpha,n_0)^{16}\mathrm{O}(0^+;\ \mathrm{gs}\ )$	(1.0, 6.5)	3,116	$\sigma, \sigma(\theta)$
$^{13}\mathrm{C}(\alpha,n_1)^{16}\mathrm{O}(0^+;\ 6.05\ \mathrm{MeV})$	(5.1, 5.6)	113	$\sigma, \sigma(\theta)$
Total		8,634	5 types

- New data
  - Ciani *et al.* (2021) $(\boldsymbol{\alpha},n_0)$
  - Brandenburg & Meisel (2021) $(\boldsymbol{\alpha},n)$
  - Febbraro, DeBoer *et al.* (2020) $(\boldsymbol{\alpha},n_0)$, $(\boldsymbol{\alpha},n_1)$

<u>17O system channel/pars</u>

- # channels: 45
  - $J^{\pi}=1/2^{\pm}, \ldots, 11/2^{\pm}$
- # parameters
  - E_λ: 81 level energies
  - $\gamma_{\lambda,c}$: 322 reduced widths
- # Normalizations
  - n_M: 95 norm scales
  - ΔE_M: 4 shift factors

^{17}O Preliminary evaluation

Preliminary results: (α,n$_0$)

13c(4he,n)16o dσ/dΩ E= 5.275 MeV

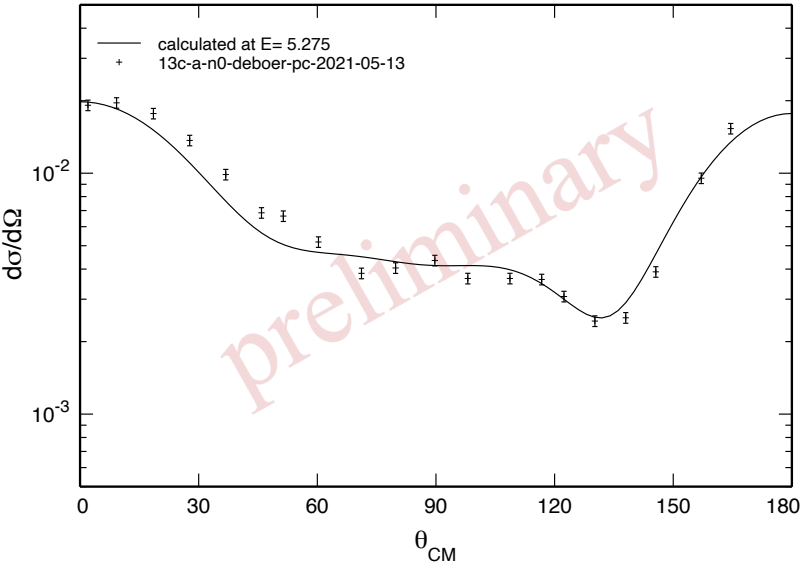

13c + 4he reaction

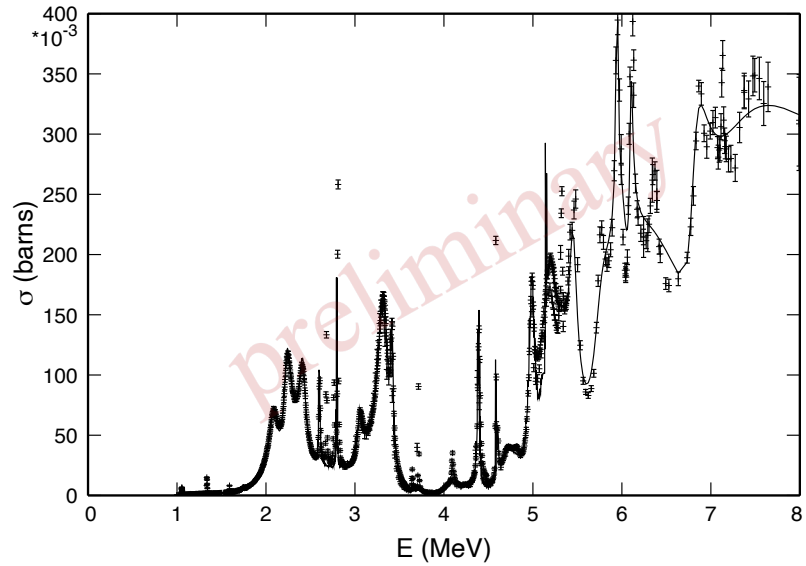

13c(4he,n)16o dσ/dΩ E= 5.895 MeV

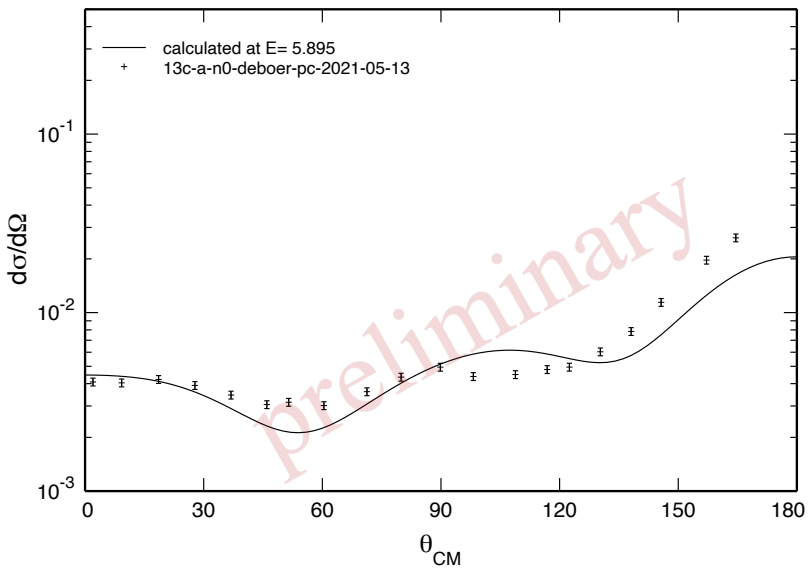

13c(4he,n)16o dσ/dΩ E= 6.504 MeV

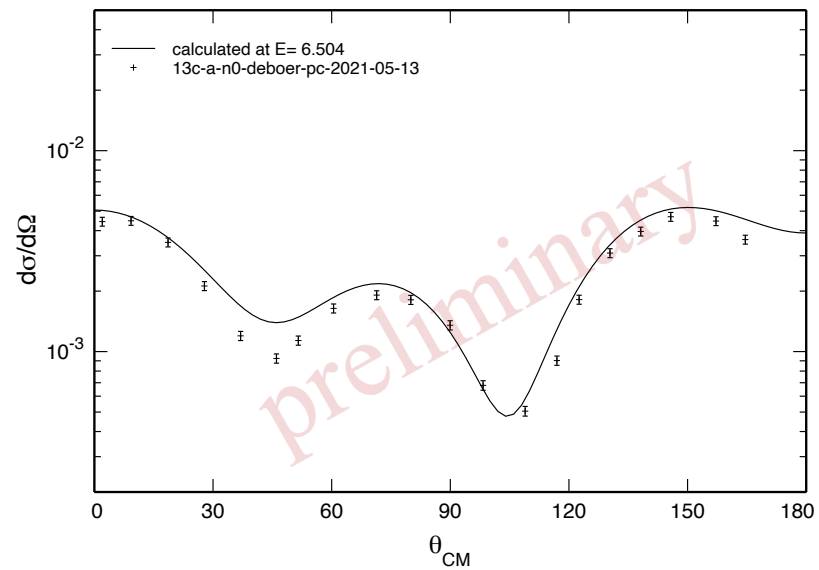

^{17}O Preliminary evaluation

Preliminary results: (α,n$_1$)

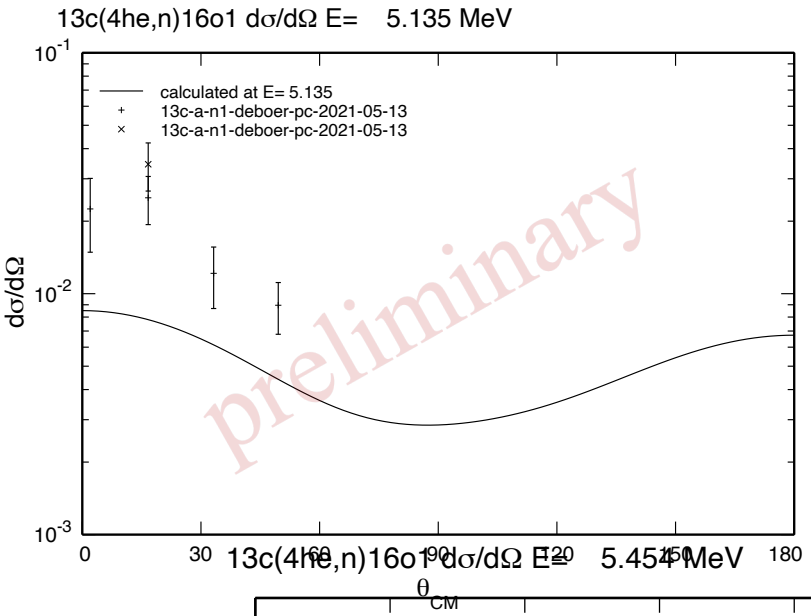

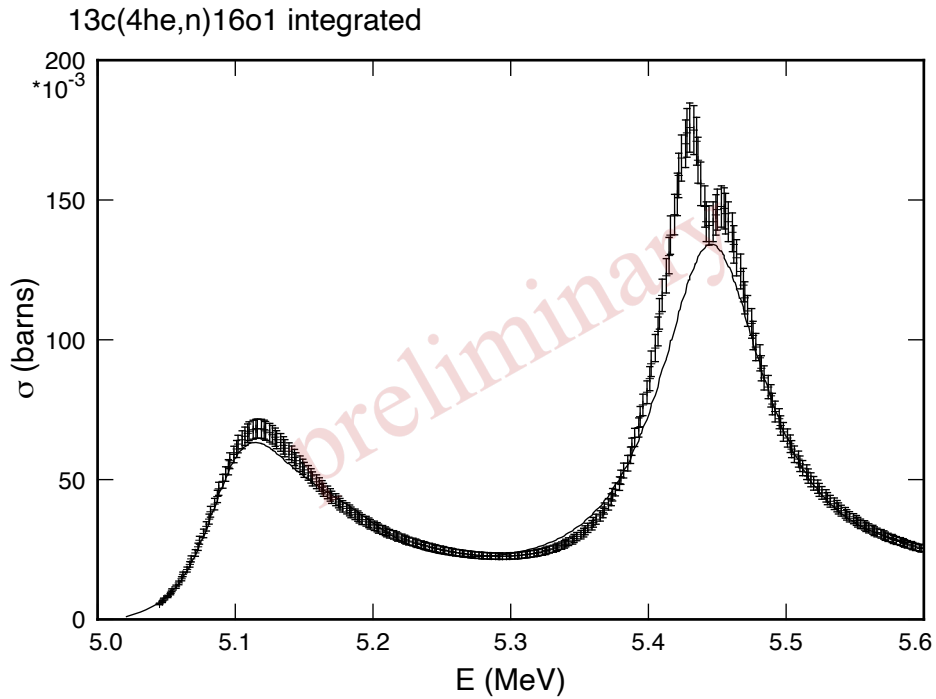

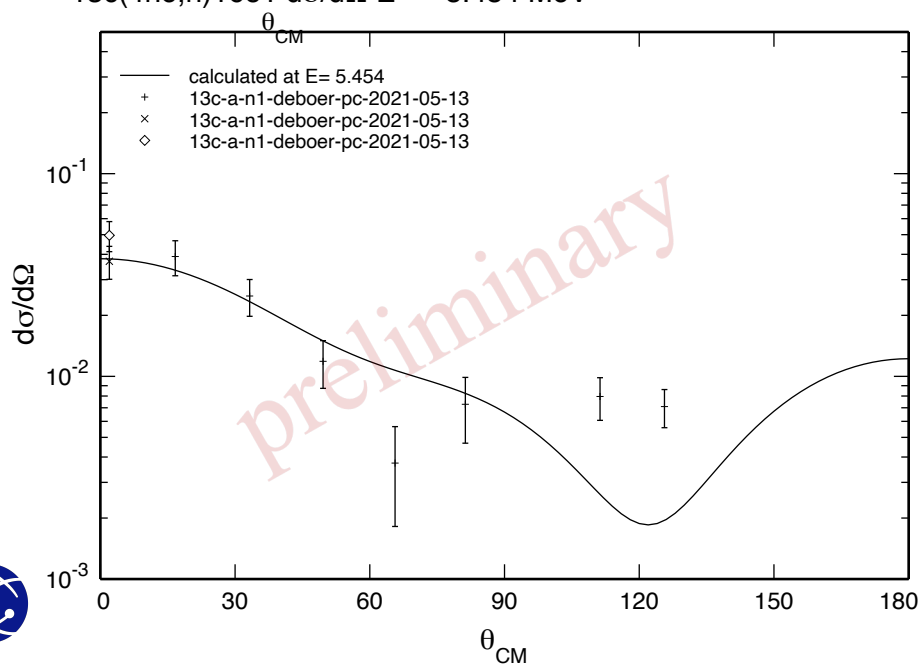

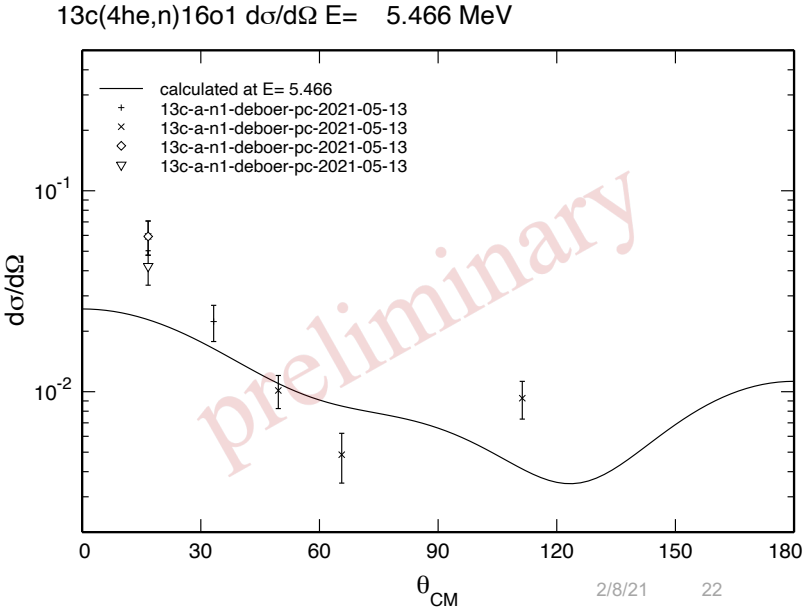

^{17}O Preliminary evaluation

Preliminary results: low energy

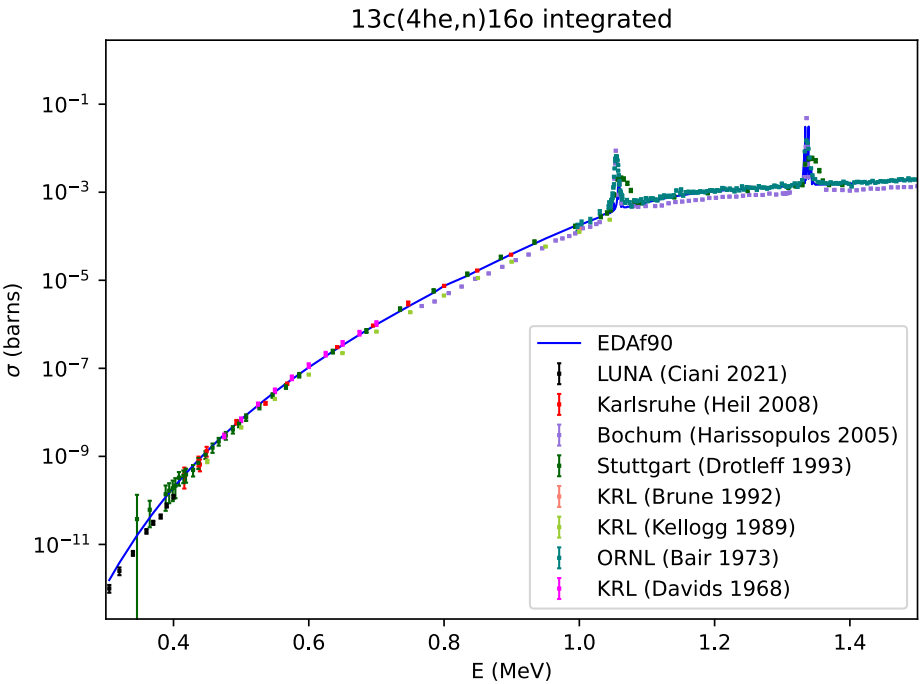

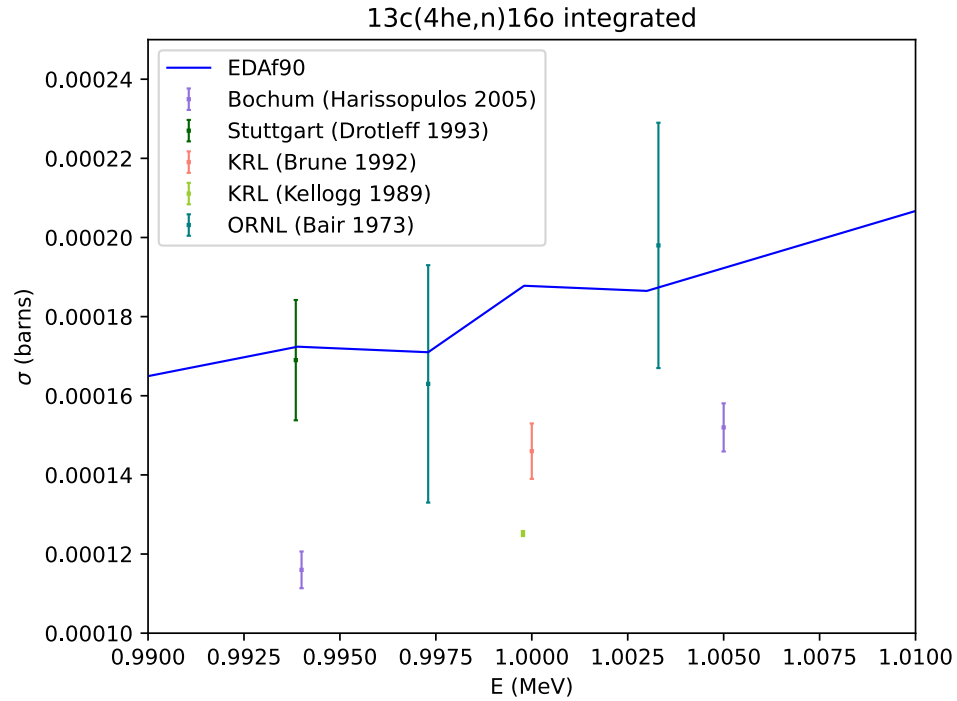

Experiment	E_α [MeV]	$\sigma_{(\alpha,n)}$ [μb]	1.000 MeV
KRL (Brune 1992)	1.0000	146(7)	146(7)
ORNL (Bair 1973)	1.0033	198(3)	179(4)
Stuttgart (Drotleff 1993)	0.9939	169(2)	187(3)
Bochum (Harissopulos 2005)	0.994	116(5)	136(7)
Bochum (Harissopulos 2005)	1.005	152(6)	–
KRL (Kellogg 1989)	0.9998	125(6)	126(8)

Measurements of $\sigma_{(\alpha,n)}(E_\alpha = 1.0$ MeV) for laboratory incident energies given in the first column, the value quoted in the second column, and the values linearly interpolated from the tabular data in the experiment's publication in the right-most column. No re-normalization factors have been applied to these values. In particular, the ORNL value of Bair & Haas[37]is quoted as originally presented without the 0.8 factor mentioned in their *Note added in proof.*

Comparison LENZ(2017) data vs. ENDF/B-VIII.0

$^{16}O(n,\alpha_0)^{13}C$ excitation functions

S. Kuvin & H.Y. Lee (LANL)

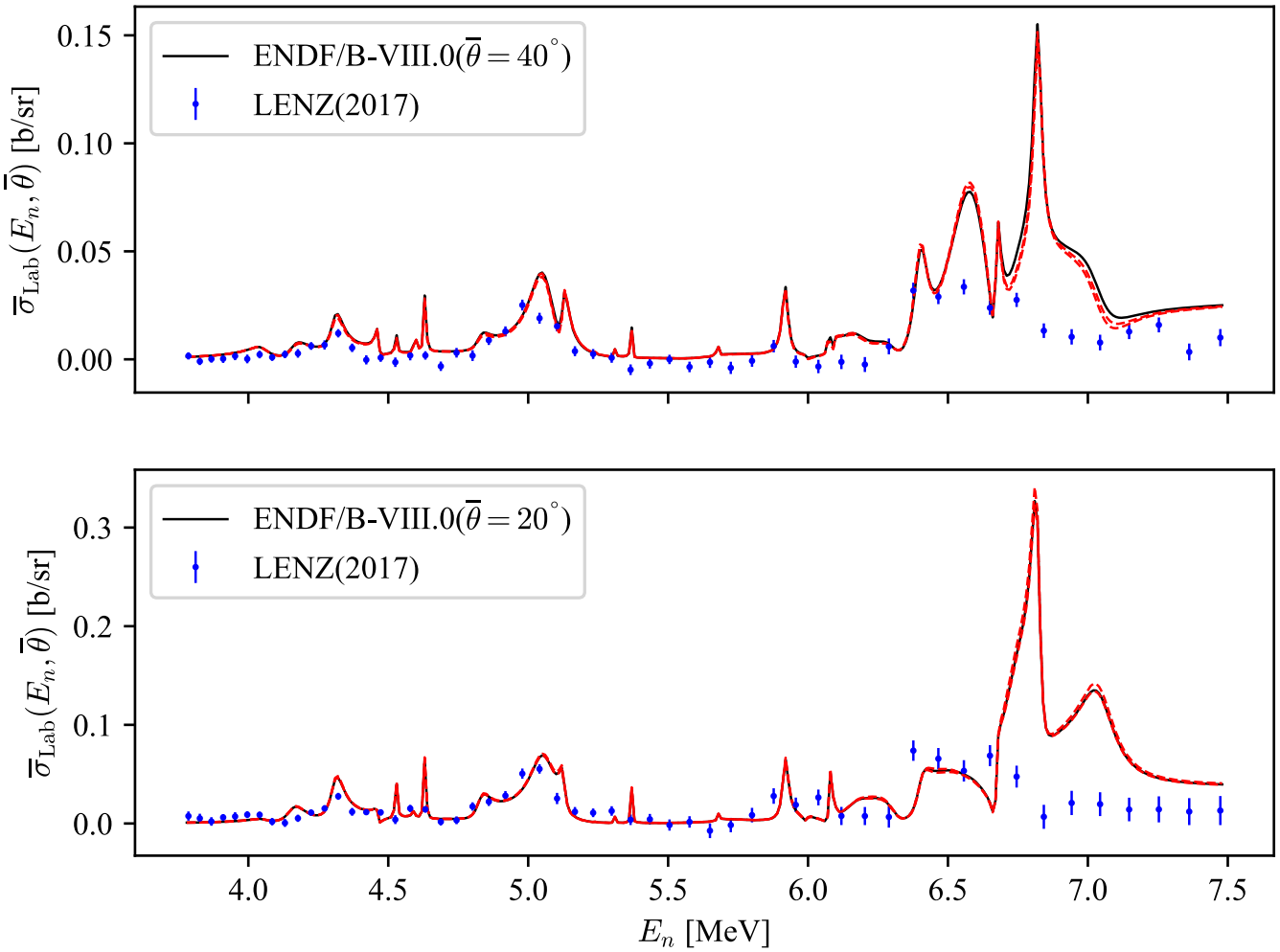

- Angular convolution
- No energy resolution broadening

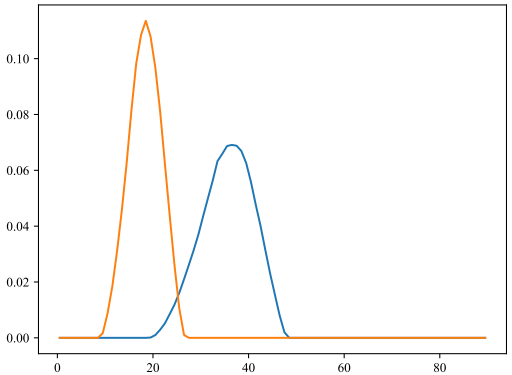

LENZ2017 acceptance vs. angle

^{17}O Preliminary evaluation scope

Preliminary results

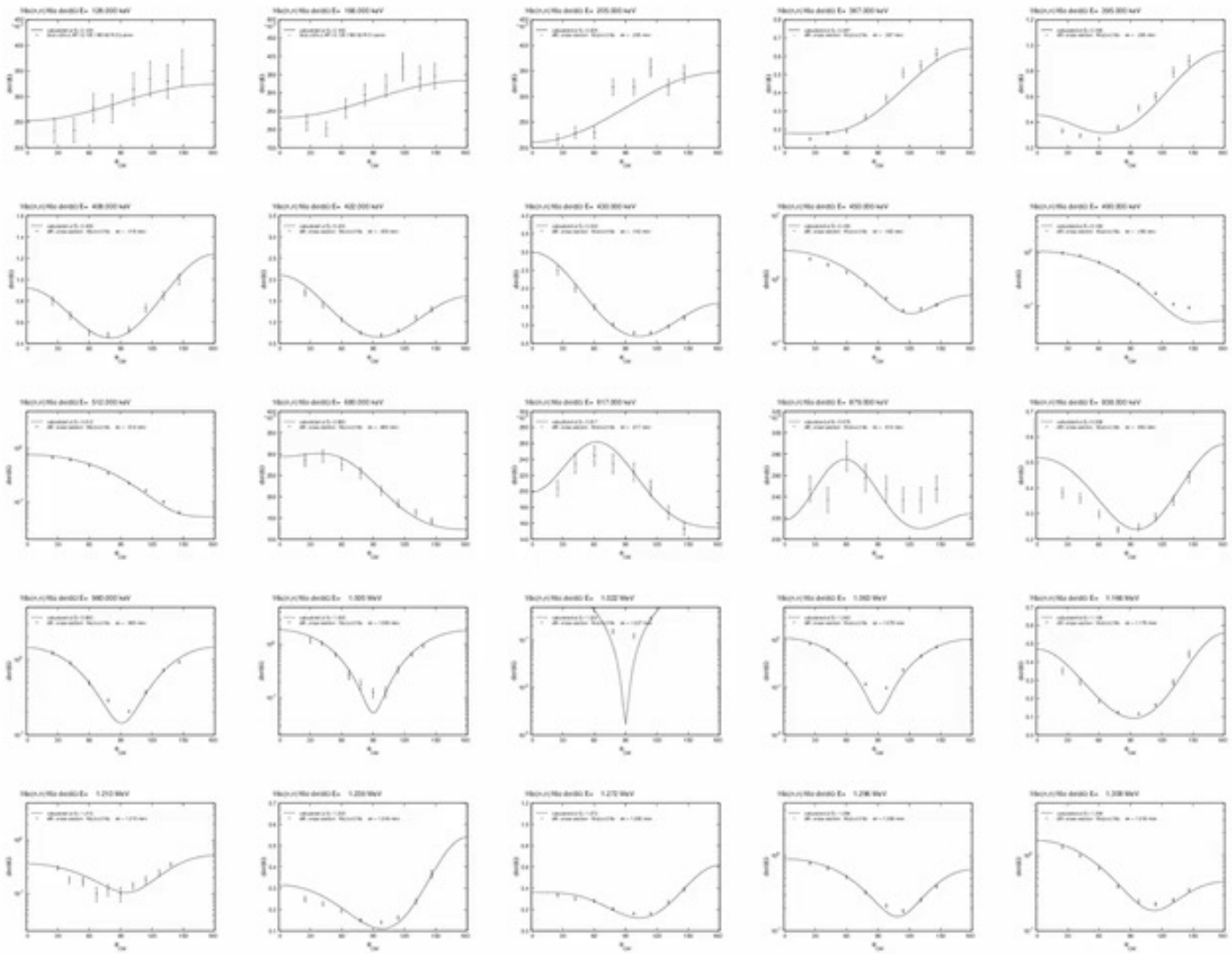

ENDF/B-VIII.0 $^{16}O(n,\alpha_0)^{13}C$ [MT=800]

Comparison with New Evaluation "8.1"

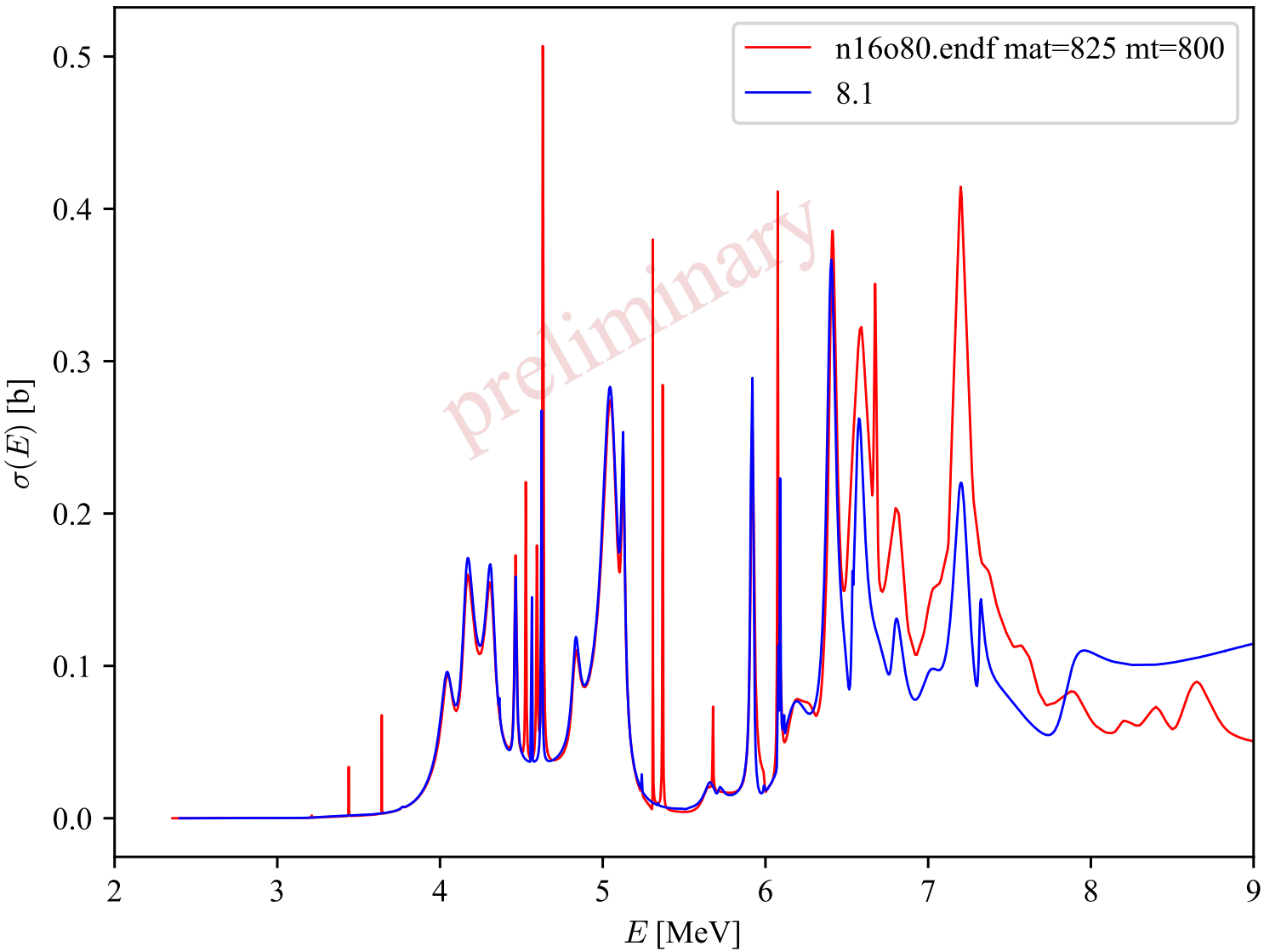

ENDF/B-VIII.0 $^{16}O(n,\alpha_0)^{13}C$ [MT=800]

Ratio of New Evaluation to ENDF/B-VIII.0

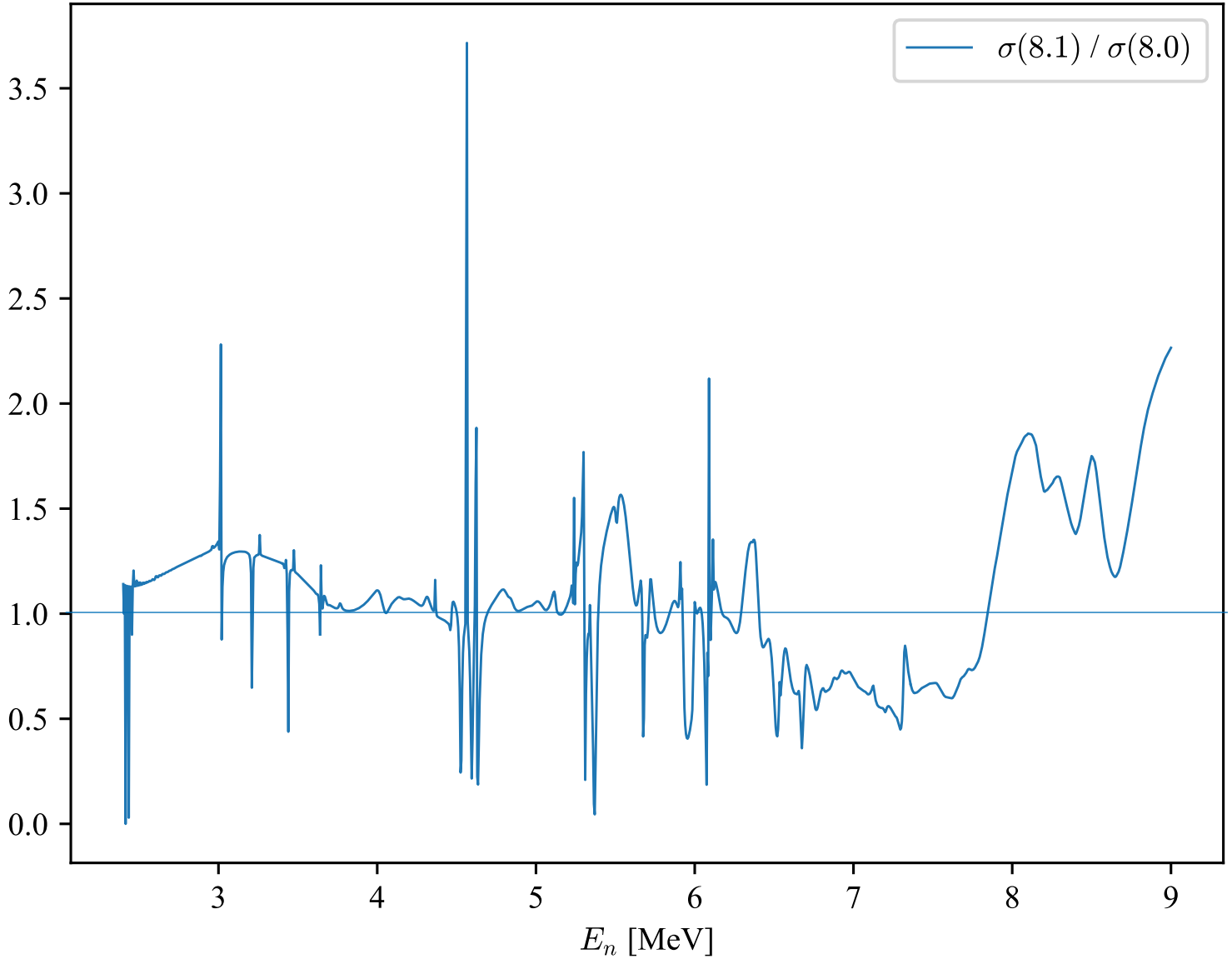

Preliminary new evaluation vs. OU(2021) & Bair & Haas(1973)

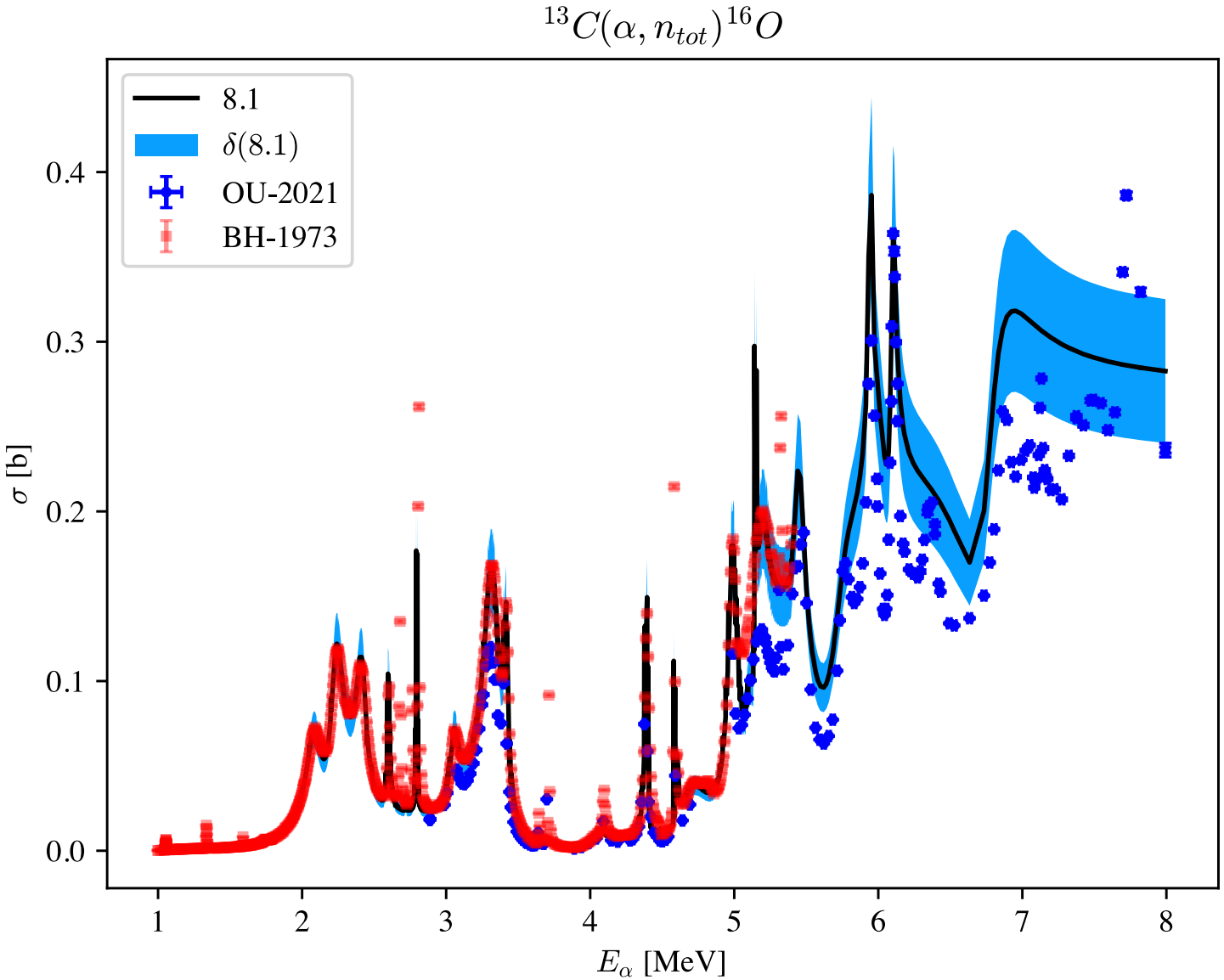

Outlook

- n+^{9}Be
  - the added inelastic data is well represented – why isn't it performing better?
    - Formatting? EDA_{f90} → ENDF-6 correct?; ENDF-6 → ACE correct?
    - Is (n,2n) properly represented?
      - ^{9}Be(n,2n)^{8}Be* vs. ^{9}Be(n,2n)$\alpha\alpha$
  - ENDF/B-VIII.1 release push to Feb. 2024
    - re-assess available data
    - push to higher energies
    - update the evaluation & covariances
- n+^{16}O
  - Complete the evaluation to E_n ~ 9 MeV (maybe 10 MeV)
    - add missing data
    - Investigate normalization of the (n,n_{tot}) Cierjacks' '68 & '83 datasets
  - ^{13}C(α,n_0)^{16}O is currently too high everywhere
    - Note that (n,n_{tot}) and (n,α_x) are tightly correlated by unitarity
  - Perform a complete normalization/covariance study